Int. J. Solids Structures Vol. 17, pp. 903–913, 1981
Printed in Great Britain.

0020-7683/81/090903-11$02.00/0
Pergamon Press Ltd.

DYNAMIC INTERACTION OF AN EMBEDDED CYLINDRICAL ROD UNDER AXIAL HARMONIC FORCES†

R. PARNES‡
Department of Solid Mechanics, Materials and Structures, School of Engineering, Tel-Aviv University, 69978 Ramat-Aviv, Israel

and

P. WEIDLINGER
Partner, Weidlinger Associates, New York, NY 10022, U.S.A.

(*Received* 24 *April* 1980; *in revised form* 8 *October* 1980)

Abstract—A model representing a pipe buried in soil is studied in order to determine the dynamic response of such a system. The model considered is represented by an embedded cylindrical rod of radius a subjected to time-harmonic longitudinal forces acting periodically at intervals L in alternating directions. (Such a loading pattern corresponds to the incoherent component of earthquake excitation.) The degree of interaction between the rod and surrounding medium as well as the amount of damping is established.

The rod and medium are assumed to behave as linear isotropic elastic materials and the interaction between the medium and rod is assumed to occur through a shear force mechanism acting at the interface. The response is found to be expressible in terms of non-dimensional ratios of density, velocity of wave propagation and an aspect ratio $a/2L$.

Results are presented in terms of dynamic amplification factors for various frequencies of the applied forces. Peak response and resonant frequencies are determined and regions where radiation damping occurs are established. A physical interpretation of the results is given.

1. INTRODUCTION

The effect of earthquakes on lifeline systems has received considerable attention in recent years[1, 2]. One question of concern is the dynamic response of pipe systems buried in soil and subjected to earthquakes. Among the most important facts to be established are the degree of interaction between the pipe and surrounding soil and the amount of damping, if any, which takes place in the system.

In this study, the response of an infinite train of pipe segments of radius a, interconnected at intervals L, is considered. The periodic, longitudinal axial forces act at the joints at intervals L. Since the relevant seismic input on the pipe is the incoherent component of the excitation[3], these forces are taken in alternating directions. The model, therefore, is assumed to be an infinite cylindrical rod embedded in an elastic medium and subjected to periodically spaced forces as shown in Fig. 1. The rod as well as the medium are assumed to behave as linear isotropic elastic materials and the interaction between the surrounding medium and rod is assumed to occur through a shear force mechanism acting at the rod–medium interface which prevents slip at this interface. Since the radial displacements of the pipe are known to be small, for mathematical simplicity, the rod is assumed to be radially rigid. Such an assumption has been used previously[4].

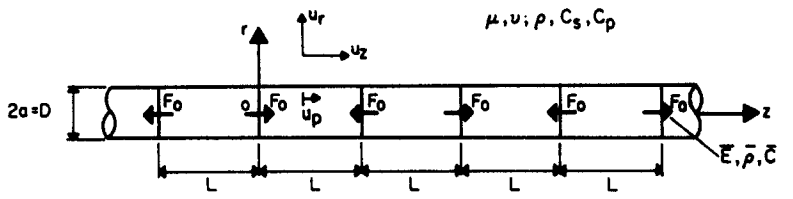

Fig. 1.

†This work was supported by the National Science Foundation under Grant PFR 78-15049 with Weidlinger Associates, New York, U.S.A.

‡Presently on leave at Laboratoire de Mécanique des Solides, Ecole Polytechnique, 91128 Palaiseau, France.

It is seen that the response can be expressed in terms of several non-dimensional ratios of density and velocity of wave propagation. The response is also seen to depend strongly on the aspect ratio $a/2L$ of the rod. Responses to several such rods are obtained as a function of the forcing frequency of the applied force.

In order to demonstrate specifically the dynamic effects, results are presented in terms of a dynamic amplification factor (DAF) defined as the ratio of dynamic to corresponding static response.

A subject of major interest is the determination of peak responses which occur at resonant frequencies. Resonance occurs when the forcing frequency coincides with the frequency of an excited wave of specific wave length in the system. (It is noted that corresponding to any given wave length, propagation can occur only at certain discrete frequencies. Such frequency-wave length relations are a result of the dispersive character of the system). Frequency ranges are established where no radiation damping occurs and it is observed that in this range, the response contains infinite DAF.

From the study of the analytic solution and observation of the numerical results obtained, several general conclusions are established which govern the response of the rod–medium system.

2. GENERAL FORMULATION AND SOLUTION

The model considered represents an infinite cylindrical rod of radius a, embedded in a medium and which is subjected to dynamic concentrated forces $F(t)$, acting in the longitudinal z-direction at periodic intervals L as shown in Fig. 1. The forces are assumed to act harmonically in time with frequency f.

The rod is represented by means of a solid cylindrical bar of cross-sectional area A with modulus of elasticity $\bar{E}$ and density $\bar{\rho}$, whose motion in the longitudinal z-direction is denoted by $U_p(z, t)$. Following the assumption of radial rigidity[4], the radial displacements are taken as zero throughout the rod.

The surrounding medium is assumed to behave as a linear elastic material having density ρ and defined by a shear modulus μ and Poisson ratio ν. For the axi-symmetric case considered here, the medium can undergo time-dependent radial and axial displacements denoted by $U_r(r, z, t)$ and $U_z(r, z, t)$ respectively.

The interaction between the rod and surrounding medium is then due to an iteractive shear force mechanism, acting along the cylindrical interface, which prevents slip between the rod and the medium.

Denoting the harmonically applied periodic concentrated forces by means of periodically spaced Dirac–delta functions $\delta_p(z)$, the force $F(t)$ is represented by

$$F(t) = F_0 \delta_p(z)\, e^{-i\omega t} \tag{1}$$

where $\omega = 2\pi f$.

The governing equation of the rod is then written as:

$$\bar{E}\frac{\partial^2 U_p(z, t)}{\partial z^2} + \frac{2\tau_{rz}(a, z, t)}{a} - \bar{\rho}\frac{\partial^2 U_p(z, t)}{\partial t^2} = -\frac{F_0}{A}\delta_p(z)\, e^{-i\omega t} \tag{2}$$

where $\tau_{rz}(a, z, t)$ represents the interactive shear stress at the interface.

With the assumptions stated above, together with the requirements on continuity of displacements at the rod–medium interface, the boundary conditions on the medium displacements become

$$U_r(a, z, t) = 0, \quad U_z(a, z, t) = U_p(z, t). \tag{3a, b}$$

The dynamic displacements of the surrounding medium, $r \geq a$ may be expressed in terms of

outgoing wave expressions (which decay as $r \to \infty$) as follows[4]:

$$U_r(r, z, t) = \sum_{m=1}^{\infty} \left[A_m \frac{h_m^*}{h^2} H_1^{(1)}(h_m^* r) + B_m \frac{\alpha_m}{k^2} H_1^{(1)}(k_m^* r) \right] \sin \alpha_m z \, e^{-i\omega t} \tag{4}$$

$$U_z(r, z, t) = \sum_{m=1}^{\infty} \left[A_m \frac{\alpha_m}{h^2} H_0^{(1)}(h_m^* r) - B_m \frac{k_m^*}{k^2} H_0^{(1)}(k_m^* r) \right] \cos \alpha_m z \, e^{-i\omega t} \tag{5}$$

where $H_0^{(1)}$ and $H_1^{(1)}$ are Hankel functions of the first kind of order zero and one respectively,

$$\alpha_m = (2m - 1)\pi / L, \tag{6}$$

$$h = \omega / c_p, \quad k = \omega / c_s, \tag{7a, b}$$

and

$$h_m^{*2} = h^2 - \alpha_m^2, \quad k_m^{*2} = k^2 - \alpha_m^2. \tag{8a, b}$$

In the above,

$$c_s = [\mu / \rho]^{1/2} \quad \text{and} \quad c_p = \left[\frac{2(1 - \nu)}{1 - 2\nu} \cdot \frac{\mu}{\rho} \right]^{1/2} \tag{9a, b}$$

are the propagation speeds in an elastic medium of outgoing S- and P-waves respectively. Thus, the terms associated with the constants A_m represent the P-waves, while the B_m terms represent the propagation of the S-waves. The constants A_m and B_m must then satisfy the boundary conditions of eqn (3).

From the first of these

$$B_m = -\left[\frac{h_m^*}{h^2} \frac{k^2}{\alpha_m} \frac{H_1^{(1)}(h_m^* a)}{H_1^{(1)}(k_m^* a)} \right] A_m. \tag{10}$$

Furthermore, since $U_r(a, z) = 0$, the shear stress at the interface is given by

$$\tau_{rz}(a, z, t) = \mu \frac{\partial U_z(a, z, t)}{\partial r} \tag{11}$$

Using the remaining boundary condition and substituting eqn (11) in eqn (2),

$$\bar{E} \frac{\partial^2 U_z(a, z, t)}{\partial z^2} + \frac{2\mu}{a} \frac{\partial U_z(a, z, t)}{\partial r} - \bar{\rho} \frac{\partial^2 U_z(a, z, t)}{\partial t^2} = -\frac{F_0}{A} \delta_p(z) \, e^{-i\omega t}. \tag{12}$$

The periodic Dirac-delta function may now be represented in the region $0 \le z \le L$ by the infinite series

$$\delta_p(z) = \frac{2}{L} \sum_{m=1}^{\infty} \cos \alpha_m z. \tag{13}$$

It is noted here in passing that the interval $0 \le z \le L$ represents a half-Fourier interval and hence the analysis of the infinite rod is given by the solution in a periodic interval $0 \le z \le \lambda$ with $\lambda = 2L$ being the total Fourier interval (see Fig. 2).

Noting that

$$\frac{dH_0^{(1)}(x)}{dx} = -H_1^{(1)}(x), \tag{14}$$

substituting the expression for U_z and its appropriate derivatives from eqn (5) and using the

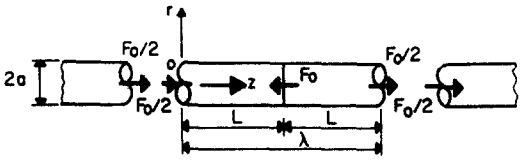

Fig. 2.

representation of eqn (13) in eqn (12), we obtain, assuming a steady-state solution, the following equation:

$$\sum_{m=1}^{\infty} A_m\left\{[\bar{E}\alpha_m{}^2-\bar{\rho}\omega^2]D_{zm}(a)-\frac{2\mu}{a}g_m\right\}\cos\alpha_m z=\frac{2F_0}{AL}\sum_{m=1}^{\infty}\cos\alpha_m z \tag{15}$$

where

$$D_{zm}(r)=\frac{\alpha_m}{h^2}H_0^{(1)}(h_m^*r)+\frac{h_m^*k_m^*}{h^2\alpha_m}\frac{H_1^{(1)}(h_m^*a)}{H_1^{(1)}(k_m^*a)}H_0^{(1)}(k_m^*r) \tag{16a}$$

and

$$g_m=\frac{\partial D_{zm}(r)}{\partial r}\bigg|_{r=a}=-\frac{h_m^*}{h^2\alpha_m}(\alpha_m{}^2+k_m^{*2})H_1^{(1)}(h_m^*a). \tag{16b}$$

By satisfying eqn (15) term by term, the constants A_m are found, after some algebraic manipulation, to be

$$A_m=\frac{1}{G_m}\frac{2F_0h^2}{\bar{E}Aa\alpha_m{}^3LH_1^{(1)}(h_m^*a)} \tag{17a}$$

where

$$G_m=\left(1-\frac{\omega^2}{\bar{c}^2\alpha_m{}^2}\right)\Lambda_m+\frac{2\mu}{\bar{E}a}\frac{h_m^*}{\alpha_m{}^4}(\alpha_m{}^2+k_m^{*2}) \tag{17b}$$

and

$$\Lambda_m=\frac{H_0^{(1)}(h_m^*a)}{H_1^{(1)}(h_m^*a)}+\frac{h_m^*k_m^*}{\alpha_m{}^2}\frac{H_0^{(1)}(k_m^*a)}{H_1^{(1)}(k_m^*a)}. \tag{17c}$$

In eqn (17),

$$\bar{c}=[\bar{E}/\bar{\rho}]^{1/2} \tag{18}$$

represents the familiar propagation velocity of longitudinal waves in a free elastic rod.

Substituting finally eqns (17) in eqn (5) and using eqn (3b), the displacement $U_p(z,t)$ is obtained; viz

$$\left(\frac{U_p}{L}\right)\left(\frac{\bar{E}A}{F_0/2}\right)=\frac{4}{\pi^2}\sum_{m=1}^{\infty}\frac{\Lambda_m\cos\alpha_m z\,e^{-i\omega t}}{(2m-1)^2G_m} \tag{19}$$

At this point it is advantageous to express the solution in terms of non-dimensional quantities and more specifically in terms of non-dimensional ratios relating the propagation velocities of the P- and S-waves in the medium and the propagation velocity $\bar{c}$ of waves in the

free bar. To this end, we define the following new non-dimensional variables:

$$\eta = a/\lambda \quad \text{where} \quad \lambda = 2L \tag{20}$$

$$\Gamma = f\lambda/\bar{c}, \tag{21}$$

and

$$R_c = c_p/c_s, \quad R_v = c_p/\bar{c}. \tag{22a, b}$$

Also, let the ratio of the densities of medium to rod be

$$R_D = \rho/\bar{\rho}. \tag{23}$$

Using these new parameters, the expression for the longitudinal displacement U_p of the bar becomes

$$\left(\frac{U_p}{L}\right)\left(\frac{\bar{E}A}{F_0/2}\right) = \frac{4}{\pi^2}\sum_{m=1}^{\infty} \frac{\cos \alpha_m z \, e^{-i\omega t}}{(2m-1)^2 - \Gamma^2\left[1 - \dfrac{2R_D\gamma_{pm}}{(2\pi\eta)^2(2m-1)^2\Lambda_m}\right]} \tag{24}$$

where now

$$\Lambda_m = \frac{H_0^{(1)}(\gamma_{pm})}{H_1^{(1)}(\gamma_{pm})} + \frac{\gamma_{pm}\gamma_{sm}}{(2\pi\eta)^2(2m-1)^2}\frac{H_0^{(1)}(\gamma_{sm})}{H_1^{(1)}(\gamma_{sm})} \tag{25}$$

in which

$$\gamma_{pm} = 2\pi\eta(2m-1)\left[\frac{\Gamma^2}{(2m-1)^2 R_v^2} - 1\right]^{1/2} \tag{26}$$

and

$$\gamma_{sm} = 2\pi\eta(2m-1)\left[\frac{R_c^2\Gamma^2}{(2m-1)^2 R_v^2} - 1\right]^{1/2}. \tag{27}$$

It is noted that the non-dimensional displacement given by eqn (24) is uniquely determined by five quantities: Γ, R_D, R_v, R_c and η.

In the above, terms containing p and s subscripts correspond to contributions from the P- and S-waves respectively. Thus, it is observed that coupling of the two wave types occurs through Λ_m given in eqn (25).

Certain limiting cases of the solution represented by eqn (24) are of particular interest.

For example, noting that

$$\lim_{R_v \to 0} \frac{\gamma_{pm}}{\Lambda_m} = 0, \tag{28}$$

the solution degenerates to

$$\left(\frac{U_p}{L}\right)\left(\frac{\bar{E}A}{F_0/2}\right) = \frac{4}{\pi^2}\sum_{m=1}^{\infty} \frac{\cos \alpha_m z \, e^{-i\omega t}}{(2m-1)^2 - \Gamma^2}. \tag{29}$$

Similarly if $R_D = 0$ or if $R_c \to \infty$ while both R_D and R_v remain finite, eqn (29) is recovered from eqn (24). The solution given by eqn (29) is recognized as the solution for a free infinite bar with no interaction, i.e. as the uncoupled solution. In all three cases such a solution is expected

since (a) $R_D = 0$ implies a massless medium (b) $R_v = 0$ implies a medium of no rigidity and (c) $R_c \to \infty$ (with R_v, R_D finite) also implies a medium of no shear rigidity since,

$$\frac{R_v^2 R_D}{R_c^2} = \mu/\bar{E}. \tag{30}$$

It is noted that for the response of the free bar, resonance occurs when

$$\Gamma = 2m - 1, \quad m = 1, 2, 3 \ldots \tag{31a}$$

i.e. when the forcing frequency f is given by

$$f = \bar{c}/\lambda, \quad 3\bar{c}/\lambda, \quad 5\bar{c}/\lambda, \quad 7\bar{c}/\lambda \ldots \tag{31b}$$

It is thus convenient to define

$$\bar{f} = \bar{c}/\lambda \tag{32}$$

which is the fundamental frequency of vibrations of the uncoupled bar, or in terms of wave propagation, the wave frequency for a longitudinal wave of wave length λ propagating in the z-direction.

The variable Γ can then be rewritten as

$$\Gamma = f/\bar{f} \tag{33}$$

and thus represents the ratio of forcing frequency to natural frequency of the uncoupled free bar. This interpretation will subsequently prove significant in understanding the results presented in the next section.

Upon taking the limit as $f \to 0$ (or $\Gamma \to 0$) of eqn (24), the static solution, identical to that obtained directly using Love strain functions[5], is recovered.

3. NUMERICAL RESULTS AND CONCLUSIONS

Numerical results are presented for the displacements of typical rods embedded in an elastic medium with a Poisson ratio $\nu = 0.25$ and for which the density ratio $R_D = \rho/\bar{\rho} = 0.2$. Results are given for a range of propagation velocity ratios and for various aspect ratios $\eta = a/\lambda$.

Significant results which demonstrate the dynamic effects on the displacements are best presented in terms of the ratio of the dynamic response U_D to the equivalent static response U_s, as obtained in[5]. The responses are therefore given in terms of the dynamic amplification factor

$$\text{DAF} = \frac{U_D(z=0)}{U_s(z=0)} \tag{34}$$

where the displacements $U_D(z=0)$ are evaluated from eqn (24). Calculations of this quantity, using $M = 15$ terms were found to insure sufficient accuracy in all cases.

Four series of results, corresponding to values $R_v = 0.5$, 1.0, 3.0 and 6.0, are presented in Figs. 3–6 respectively.† For each series, the response for aspect ratios $\eta = a/\lambda = 0.01, 0.02, 0.05$ and 0.1 is found.

The responses are presented as a function of $\Gamma = f/\bar{f}$, for $0 \le \Gamma \le 10$, with the other parameters held fixed. Analogously to the definition of $\bar{f}$ (as given in eqn 32), it is appropriate to

†These values of R_v were used in an attempt to simulate the properties of jointed pipes. (Choosing low values of $\bar{E}$ to represent the effect of the flexible joints, yields low values of $\bar{c}$ according to eqn (18) and hence relatively large values for R_v.) A subsequent study, using a more refined model for jointed pipes[6] has shown that the use of a low "global modulus" $\bar{E}$ cannot adequately represent the realistic conditions of relatively rigid pipes embedded in typical soils.

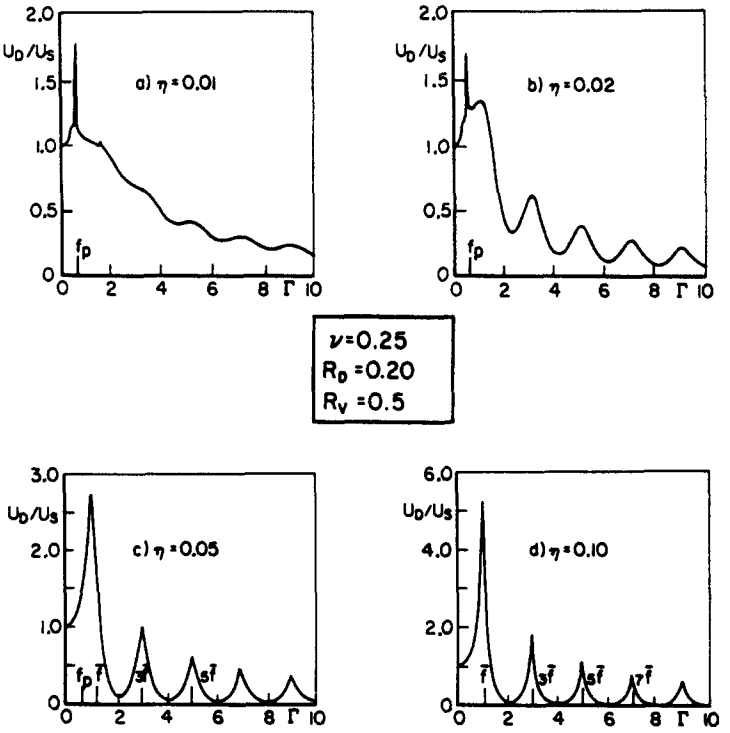

Fig. 3. Displacements, $R_v = 0.5$.

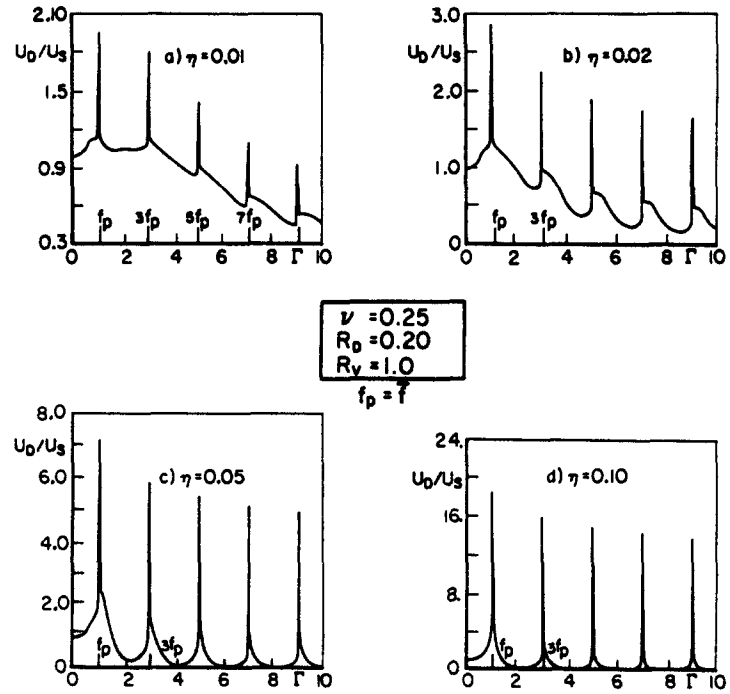

Fig. 4. Displacements, $R_v = 1.0$.

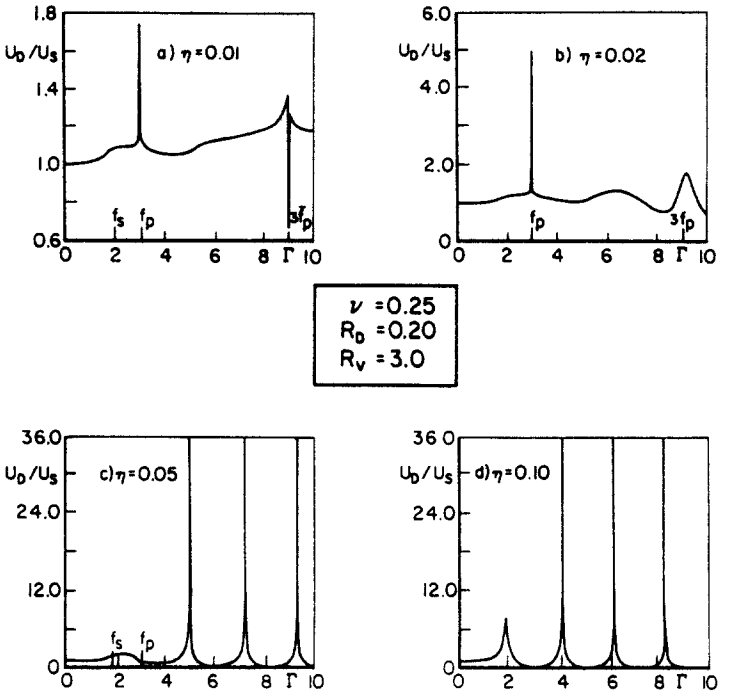

Fig. 5. Displacement, $R_v = 3.0$.

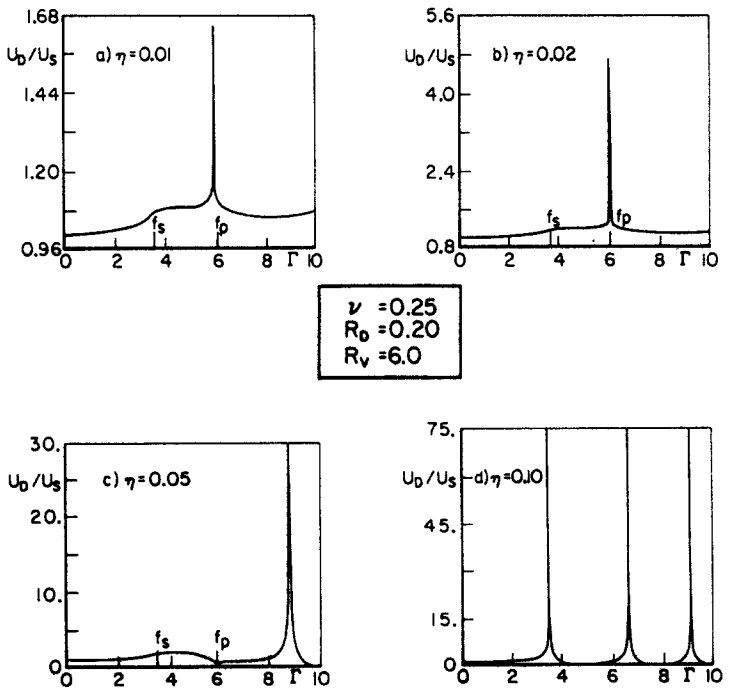

Fig. 6. Displacements, $R_v = 6.0$.

define the equivalent wave frequency of the S- and P-waves propagating in the medium by

$$f_s = c_s/\lambda, \quad f_p = c_p/\lambda \tag{35}$$

respectively. These frequencies are indicated in all figures presented below. It should be noted that from their definitions, $f_p = \bar{f}R_e$.

In considering the results presented in these figures, we shall first concentrate, in particular, on the influences of the aspect ratio and point out certain features which, as will be seen in the discussion which follows, are explicable in terms of the existence or inexistence of radiation damping which can occur in the system.

To this end, it is first noted from Fig. 3, with $R_e = 0.50$, that all displacements are finite, although sharp finite peaks do occur. For $\eta = 0.01$ and 0.02, a sharp peak occurs at $f = f_p$, while for greater values of $\eta(\eta = 0.05$ and 0.1) sharp but finite peaks occur at $f \doteq n\bar{f}$, $(n = 1, 3, 5 \ldots)$ as indicated along the abscissa. In general, since $\bar{f}$ is an intrinsic property of the rod, we may conclude that with increasing values of η, the rod properties tend to predominate while for smaller η the embedding medium is more effective. Moreover, the peak displacements are seen to increase considerably with increasing values of η. From both of these observations, we may thus conclude that the interaction at the rod–medium interface is significantly weakened with increasing values of η, i.e. when L decreases. This effect is in accord with the results found for the corresponding static case[5].

If Fig. 4, we observe a similar behavior for $R_e = 1.0$, (for which $f_p = \bar{f}$) and note again that finite peaks occur at $f \doteq nf_p = n\bar{f}$ $(n = 1, 3, 5 \ldots)$. These finite peaks are again seen to increase with greater values of η. In anticipation of the discussion below, we shall refer to these finite peaks as "damped resonant" behavior.

From Fig. 5 with $R_e = 3.0$, we note two types of response: for small values of $\eta(\eta = 0.01$ and 0.02) abrupt changes of behavior occur at frequencies $f = f_p, 3f_p$. However being finite, they again describe a damped resonant behavior. For larger values of η, $(\eta = 0.05$ and 0.1) both finite peaks and infinite responses, corresponding to true resonance, occur. Thus, e.g. in Fig. 5d, a finite peak response occurs at $f \sim 1.83\ \bar{f}$, while infinite peaks exist for certain discrete values of $f/\bar{f}$. The different kinds of response occuring here are analyzed and explained below.

In Fig. 6 with $R_e = 6.0$, we again note a relatively smooth behavior except for damped resonance for $\eta = 0.01$ and $\eta = 0.02$, which occurs at $f = f_p$, while for larger values of η infinities exist for discrete values of Γ.†

We now turn our attention to an analysis of the results, and in particular to an explanation of the damped (finite) and undamped (infinite) resonant responses.

It is first observed that infinite responses can only occur if a particular m term of the denominator of eqn (24) vanishes. The vanishing of such a denominator establishes the dispersion relation of the system, relating the frequency f to a/λ, i.e. the vanishing of this term is equivalent to the frequency equation which determines the dispersion relations. In a previous paper[7], it is shown that real roots of the frequency equation can only exist if $\bar{c} < c_s$, or in terms of the parameters defined by eqns (22), the denominator can vanish (and therefore infinite responses can exist) only if

$$\frac{R_e}{R_c} \equiv \left[\frac{2(1-\nu)}{1-2\nu}\right]^{1/2} R_e > 1. \tag{36}$$

For $\nu = 0.25$, we therefore observe that for $R_e < \sqrt{3}$, no infinites can occur. The results presented in Figs. 3 and 4, with $R_e = 0.5$ and 1.0 respectively, correspond to this case; all peak responses were indeed observed to be finite. On the other hand, in Figs. 5 and 6, R_e is such that infinite resonance can occur, since possible roots of the frequency equations can exist. However, we note for example in Fig. 5d that the first peak at $f \sim 1.837$ is finite while the

†For typical buried pipelines (having material relatively stiffer than the surrounding medium and containing joints which are small relative to the length of pipe segments) it may be concluded that resonant or near resonant behavior does not occur for frequencies in the earthquake range. Hence Figs. 3–6, based on relatively large values of R_e, should not be construed as representing typical earthquake behavior (see previous footnote).

remaining peaks (occuring at $f/\bar{f} \sim 4.13$, 6.195, 8.26) are infinite. Thus the criteria, $R_v > \sqrt{3}$ is not sufficient to ensure that all peaks will be infinite. In order to understand this difference in behavior, it is worthwhile, at this point, to examine the mathematical nature of the solution, from which it is possible to establish ranges of frequencies where radiation damping can occur in the system.

An understanding of the basic damping mechanism and resonant response is best obtained by examining eqns (4) and (5) which define the displacements of points in the surrounding medium. From these equations, it is observed that the displacement expressions contain terms of the nature $H_n^{(1)}(h_m^* r)\,e^{-i\omega t}$ and $H_n^{(1)}(k_m^* r)\,e^{-i\omega t}$, $n = 0$ and 1, where h_m^* and k_m^* are originally defined by eqns (8). In terms of the new parameters given by eqns (20)–(22), (32) and (35), h_m^* and k_m^* are expressed respectively by

$$h_m^* = \frac{2\pi}{\lambda}\left[\frac{\Gamma^2}{(f_p/\bar{f})^2} - (2m-1)^2\right]^{1/2} \tag{37a}$$

and

$$k_m^* = \frac{2\pi}{\lambda}\left[\frac{\Gamma^2}{(f_s/\bar{f})^2} - (2m-1)^2\right]^{1/2}. \tag{37b}$$

Thus, if $\Gamma > (2m-1)f_p/\bar{f}$, h_m^* is real, while if $\Gamma < (2m-1)f_p/\bar{f}$, h_m^* is imaginary. (Similar conclusions exist for k_m^* upon replacing f_p by f_s.).

In the case where h_m^* and k_m^* are real, the response is expressed in terms of Hankel functions of real arguments. Such terms then represent outward propagating waves in which energy is continuously propagated outwardly by the respective P- and S-waves. Thus, there exists, due to the outward radiation, a damping mechanism, and the system experiences radiation damping.

On the other hand, if the arguments of the Hankel functions are imaginary, the Hankel functions, in effect, are transformed into K_n Bessel functions according to the relation[8]

$$H_n^{(1)}(ix) = \frac{2i^{-(n+1)}}{\pi} K_n(x). \tag{38}$$

The response, expressed then in terms of K_n funciions, no longer is represented by radiating waves. Hence, no radiation of energy can take place and the system can experience no radiation damping.

Since the above discussion is applicable to both the h_m^* and k_m^* terms which correspond respectively to P- and S-waves, the following may be concluded:†

(a) If $(2m-1)f_p/\bar{f} \leq \Gamma$, radiation damping will take place through both the P- and S-wave mechanism.

(b) If $(2m-1)f_s/\bar{f} \leq \Gamma < (2m-1)f_p/\bar{f}$, radiation damping will take place only through the S-wave mechanism.

(c) If $\Gamma < (2m-1)f_s/\bar{f}$, no radiation damping can take place.

Thus peaks which occur at values of Γ which satisfy conditions (a) or (b) above, are always finite since they correspond to a damped resonance while if Γ satisfies condition (c) the peaks will be infinite, describing an undamped resonant system.

Returning now to Fig. 5(d), for which $f_s/\bar{f} = \sqrt{3}$, we note that the first peak occuring at $\Gamma \sim 1.83 > \sqrt{3}$ does not satisfy condition (c) for $m = 1$ and hence the peak is necessarily finite. On the other hand, the remaining three values of Γ at which peaks occur correspond to values $m = 2, 3$ and 4 respectively and thus, satisfying condition (c) above, infinite peaks occur at these values.

†These conclusions are in accord with the results of [7] where it is shown that real roots of the frequency equation will always be within the range $\bar{f} \leq f < f_s$.

In conclusion, the behavior may be interpreted in physical terms. It is first noted that, upon substituting eqns (4) and (13) in eqn (1), the applied force is represented by

$$F(t) = \frac{2F_0}{L} e^{-i\omega t} \sum_{m=1}^{\infty} \cos \frac{(2m-1)\pi z}{L}. \tag{39}$$

Hence we observe that for a steady state solution to exist, applied forces with frequency ω excite waves of wave length λ, $\lambda/3$, $\lambda/5 \ldots$ where $\lambda = 2L$. We recall too that for a system governed by a prescribed set of parameters, eqns (20)–(23), waves of a given wave length λ may propagate freely with certain discrete frequencies f according to the existing dispersion relations of the system [7].

Now, if the frequency of the applied forces $f = \omega/2\pi$ coincides with the prescribed discrete frequency of one of the excited waves of length λ, $\lambda/3$, $\lambda/5 \ldots \lambda/(2m-1)a \ldots$, resonance will occur with no damping. If, on the other hand, the parameters of the system are such that there can be no coincidence between the applied frequency and the "natural frequency" of the excited wave, then the response will be smooth or at most, a damped resonance will occur.

REFERENCES

1. *Proc. U.S.-Japan Seminar on Earthquake Engng Research With Emphasis on Lifeline Systems.* Tokyo (1976).
2. The current state of knowledge of lifeline earthquake engineering. *Proc. Tech. Council on Lifeline Earthquake Engng Specialty Conf.*, University of California at Los Angeles, ASCE (1977).
3. P. Weidlinger and I. Nelson, Seismic analysis of pipelines with interference response spectra. *NSF Grant Rep.* GR-7, Weidlinger Associates (June 1978).
4. K. Toki and S. Takada, Earthquake response analysis of underground tubular structures. *Bull. Disas. Prev. Res. Inst.* 24(221), Kyoto University (June 1964).
5. R. Parnes, Response of an elastically embedded rod subjected to periodically spaced longitudinal forces. *Int. J. Solids Structures* (in Press).
6. J. P. Wright and S. Takada, Earthquake response characteristics of jointed and continuous buried lifelines. *Proc. 7th World Conf. on Earthquake Engng*, Vol. 8, pp. 281–286. Istanbul, Turkey (Sept. 1980).
7. R. Parnes, Dispersion relations of a rod embedded in an elastic medium. *J. Sound Vibr.* 75(4) (1981).
8. N. W. McLachlan, *Bessel Functions for Engineers*, Oxford (1955).